Heuristic Algorithms for Placing Geomagnetically Induced Current Blocking Devices

Minseok Ryu*, Ahmed Attia†, Arthur Barnes‡, Russell Bent§, Sven Leyffer†, and Adam Mate‡

*School of Computing and Augmented Intelligence
Arizona State University, Tempe, AZ

†Mathematics and Computer Science Division
Argonne National Laboratory, Lemont, IL

‡Information Systems and Modeling Group and §Applied Mathematics and Plasma Physics Group
Los Alamos National Laboratory, Los Alamos, NM

***Abstract*—We propose a new heuristic approach for solving the challenge of determining optimal placements for geomagnetically induced current blocking devices on electrical grids. Traditionally, these determinations are approached by formulating the problem as mixed-integer nonlinear programming models and solving them using optimization solvers based on the spatial branch-and-bound algorithm. However, computing an optimal solution using the solvers often demands substantial computational time due to their inability to leverage the inherent problem structure. Therefore, in this work we propose a new heuristic approach based on a three-block alternating direction method of multipliers algorithm, and we compare it with an existing stochastic learning algorithm. Both heuristics exploit the structure of the problem of interest. We test these heuristic approaches through extensive numerical experiments conducted on the EPRI-21 and UIUC-150 test systems. The outcomes showcase the superior performance of our methodologies in terms of both solution quality and computational speed when compared with conventional solvers.**

***Index Terms*—geomagnetic disturbance, geomagnetically induced current mitigation, blocking devices, heuristic approaches, mixed-integer nonlinear programs.**

I. Introduction

This paper considers a geomagnetically induced current (GIC) blocking device placement problem, referred to herein as the GIC-BDP problem, for determining optimal locations for installing a limited number of devices to mitigate the adverse effect of GIC on transmission networks. The blocking device consists of standard distribution capacitors intended to block the flow of GIC by disconnecting a neutral grounding impedance [1]. As these devices are expensive, it is imperative to adopt a selective approach to their placement. It is worth mentioning that the placement itself presents a challenge due to the potential for installing a blocking device at one location to exacerbate GIC levels at others across the power grid [2]. Consequently, simplistic strategies like greedy methods are likely inadequate in this scenario. This motivates the optimization-driven placement methodologies to inform decisions regarding the placement of blocking devices.

GICs are low-frequency currents that can flow through transmission lines and transformers, which typically emerge because of a substantial electric field present on the Earth's surface, often referred to as the E-field. The increase in E-field strength often stems from naturally occurring geomagnetic disturbances (GMDs) induced by severe space weather events or from intentional electromagnetic pulse (EMP) attacks, visualized in Fig. 1.

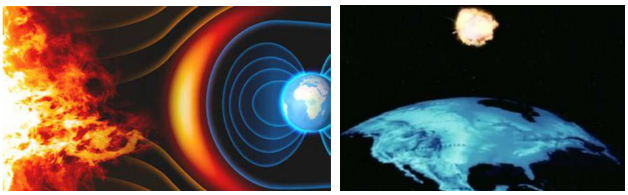

Fig. 1: Visualization of GMD (left) and EMP (right) by the U.S. Department of Homeland Security [3].

The presence of GIC can give rise to various adverse effects, including the emergence of current harmonics, transformer saturation, and increased reactive power losses. Each of these has the potential to cause damage to critical equipment and even trigger cascading failures [4]–[6]. Considering the severity of these consequences, mitigating the flows of GIC holds significant importance in ensuring the resilience and reliability of bulk energy systems. A handful of potential strategies for GIC mitigation have been put forth in the literature [2], [7]: installation of blocking devices [1], [8]–[14] and employing transmission line switching [15]–[17]. The optimization of these mitigation approaches is often formulated as a mixed-integer nonlinear programming (MINLP) model. Optimal solutions to these models can be computed by using techniques such as the spatial branch-and-bound algorithm, as demonstrated in [10]. This process can be time-consuming, however, mainly due to the presence of (i) binary variables that determine the placement of blocking devices or the selection of switched-on transmission lines, (ii) absolute-value equations used for computing the effective GIC, and (iii) nonlinear, nonconvex equations containing trilinear terms that involve trigonometric functions for computing AC optimal power flow (OPF) on transmission networks.

In this paper we reformulate the MINLP model for the GIC-

BDP problem and propose a heuristic approach that provides good-quality solutions within reasonable computation time. Our contributions are summarized as follows:

1) We reformulate the absolute-value equations as complementarity constraints [18]–[20] in the MINLP model to avoid potential convergence failure in MINLP solvers.
2) We propose a three-block alternating direction method of multipliers (ADMM) algorithm for solving the MINLP model, where the first-block subproblem is an integer program that admits a closed-form solution and the second- and third-block subproblems are NLPs.
3) For comparison, we adapt a stochastic learning (SL) algorithm for solving the MINLP model, which samples binary variables from a joint multivariate Bernoulli distribution whose parameters are optimized iteratively.

The remainder of this paper is organized as follows. In Section II we present our MINLP model for the GIC-BDP problem. In Section III we present two heuristic approaches that exploit the structure of the problem. In Section IV we show that our heuristic approaches outperform the state-of-the-art MINLP solvers with respect to solution quality and computation speed.

II. AC-OPF and GIC Blocker Model

Here we present a MINLP model for the GIC-BDP problem that determines optimal locations for installing a limited quantity of devices to effectively mitigate the detrimental effects of GIC on transmission networks. In contrast to preceding studies [15], [17], which relied on the polar representation of power flow, the rectangular form of power flow equation is embedded in our model to avoid potential numerical instability of MINLP solvers, primarily attributed to the presence of trilinear terms that involve trigonometric functions within the polar form.

In what follows, we briefly describe each set of constraints in our MINLP model.

1) Operational constraints:

$$f_k^{\mathrm{p}} \in [\underline{f}_k^{\mathrm{p}}, \overline{f}_k^{\mathrm{p}}], \quad f_k^{\mathrm{q}} \in [\underline{f}_k^{\mathrm{q}}, \overline{f}_k^{\mathrm{q}}], \ \forall k \in \mathcal{G}, \tag{1a}$$

$$v_i^{\mathrm{R}} \in [\underline{v}_i^{\mathrm{R}}, \overline{v}_i^{\mathrm{R}}], \quad v_i^{\mathrm{I}} \in [\underline{v}_i^{\mathrm{I}}, \overline{v}_i^{\mathrm{I}}] \ \forall i \in \mathcal{N}, \tag{1b}$$

$$p_{ei}^2 + q_{ei}^2 \le (\overline{s}_e)^2, \quad p_{ej}^2 + q_{ej}^2 \le (\overline{s}_e)^2, \ \forall e_{ij} \in \mathcal{E}, \tag{1c}$$

where $\mathcal{G}$, $\mathcal{N}$, $\mathcal{E}$ represent sets of generators, buses and lines within an AC network, respectively. In Eq. (1a), f_k^{p} and f_k^{q} are variables representing the real and reactive power generated by a generator $k \in \mathcal{G}$, respectively. These variables are constrained to lie within the intervals $[\underline{f}_k^{\mathrm{p}}, \overline{f}_k^{\mathrm{p}}]$ and $[\underline{f}_k^{\mathrm{q}}, \overline{f}_k^{\mathrm{q}}]$, respectively. In Eq. (1b), v_i^{R} and v_i^{I} are variables representing the real and imaginary parts of the complex voltage at bus $i \in \mathcal{N}$, respectively. These variables are bounded within the intervals $[\underline{f}_k^{\mathrm{p}}, \overline{f}_k^{\mathrm{p}}]$ and $[\underline{f}_k^{\mathrm{q}}, \overline{f}_k^{\mathrm{q}}]$, respectively. In Eq. (1c), (p_{ei}, p_{ej}) and (q_{ei}, q_{ej}) are variables representing the real and reactive power flow on line $e_{ij} \in \mathcal{E}$, respectively. The apparent power flow on each line $e \in \mathcal{E}$ should satisfy its limit $\overline{s}_e$.

2) Power flow equations: For every line $e_{ij} \in \mathcal{E}$, we have

$$p_{ei} = g_e w_i - (g_e w_e^{\mathrm{c}} + b_e w_e^{\mathrm{s}}), \tag{2a}$$

$$p_{ej} = g_e w_j - (g_e w_e^{\mathrm{c}} - b_e w_e^{\mathrm{s}}), \tag{2b}$$

$$q_{ei} = -(b_e + b_e^{\mathrm{c}}/2) w_i + (b_e w_e^{\mathrm{c}} - g_e w_e^{\mathrm{s}}), \tag{2c}$$

$$q_{ej} = -(b_e + b_e^{\mathrm{c}}/2) w_j + (b_e w_e^{\mathrm{c}} + g_e w_e^{\mathrm{s}}), \tag{2d}$$

where g_e, b_e, and b_e^{c} are conductance, susceptance, and line-charging susceptance of line $e \in \mathcal{E}$, respectively, and

$$w_i = v_i^{\mathrm{R}} v_i^{\mathrm{R}} + v_i^{\mathrm{I}} v_i^{\mathrm{I}}, \ \forall i \in \mathcal{N}, \tag{2e}$$

$$w_e^{\mathrm{c}} = v_i^{\mathrm{R}} v_j^{\mathrm{R}} + v_i^{\mathrm{I}} v_j^{\mathrm{I}}, \ \forall e_{ij} \in \mathcal{E}, \tag{2f}$$

$$w_e^{\mathrm{s}} = v_j^{\mathrm{R}} v_i^{\mathrm{I}} - v_i^{\mathrm{R}} v_j^{\mathrm{I}}, \ \forall e_{ij} \in \mathcal{E}, \tag{2g}$$

$$\tan(\underline{\theta}_{ij}) w_e^{\mathrm{c}} \le w_e^{\mathrm{s}} \le \tan(\overline{\theta}_{ij}) w_e^{\mathrm{c}}, \tag{2h}$$

which ensure that power flow is governed by Ohm's law. Note that $\underline{\theta}_{ij}$ and $\overline{\theta}_{ij}$ are lower and upper bounds on the phase angle difference at $e_{ij} \in \mathcal{E}$.

3) Balance equations with reactive power losses by GIC: For every bus $i \in \mathcal{N}$, we are given sets $(\mathcal{G}_i, \mathcal{E}_i)$ of generators and lines connected to the bus i, power demand $(d_i^{\mathrm{p}}, d_i^{\mathrm{p}})$, and shunt conductance and susceptatnce $(g_i^{\mathrm{s}}, b_i^{\mathrm{s}})$. The balance equations can be written as follows:

$$\sum_{e \in \mathcal{E}_i} p_{ei} = \sum_{k \in \mathcal{G}_i} f_k^{\mathrm{p}} - d_i^{\mathrm{p}} + l_i^{\mathrm{p+}} - l_i^{\mathrm{p-}} - g_i^{\mathrm{s}} w_i, \tag{3a}$$

$$\sum_{e \in \mathcal{E}_i} q_{ei} = \sum_{k \in \mathcal{G}_i} f_k^{\mathrm{q}} - d_i^{\mathrm{q}} + l_i^{\mathrm{q+}} - l_i^{\mathrm{q-}} + b_i^{\mathrm{s}} w_i - d_i^{\mathrm{qloss}}, \tag{3b}$$

where $(l_i^{\mathrm{p+}}, l_i^{\mathrm{q+}})$ are real and reactive power load shedding, and $(l_i^{\mathrm{p-}}, l_i^{\mathrm{q-}})$ are real and reactive power overconsumed. Note that d_i^{qloss} represents reactive power losses by GIC, computed by

$$d_i^{\mathrm{qloss}} = \sum_{e \in \mathcal{E}_i^{\tau}} K_e \sqrt{w_i} I_e^{\mathrm{eff}}, \ \forall i \in \mathcal{N}, \tag{4a}$$

$$I_e^{\mathrm{eff}} \in [0, \overline{I}_e], \ \forall e \in \mathcal{E}^{\tau}, \tag{4b}$$

where $\mathcal{E}^{\tau}$ is a set of transformers, $\mathcal{E}_i^{\tau}$ is a set of transformers connected to bus $i \in \mathcal{N}$, K_e is a loss factor, $\overline{I}_e$ is an upper limit of the effective GIC, I_e^{eff} is the amounts of effective GIC at a transformer $e \in \mathcal{E}^{\tau}$, which are computed utilizing a representative DC network $(\mathcal{N}^{\mathrm{d}}, \mathcal{E}^{\mathrm{d}})$ derived from modifications made to the original AC network $(\mathcal{N}, \mathcal{E})$, as shown in Fig. 2.

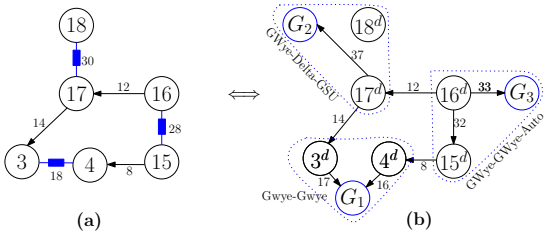

Fig. 2: AC (left) and DC (right) power network [17].

4) GIC Model: The DC network is constructed by adding a set of substations (e.g., G_1, G_2, and G_3 in Fig. 2) to the underlying AC network. For each line of the DC network, the

GIC-induced voltage source is given by ξ_ℓ, which is zero for all transformers (e.g., line numbers 16, 17, 32, 33, and 37 in Fig. 2) and has nonzero values for all transmission lines. With this information, the GIC can be computed as

$$I^{\mathrm{d}}_\ell = \gamma_\ell (v^{\mathrm{d}}_m - v^{\mathrm{d}}_n + \xi_\ell),\ \forall \ell_{mn} \in \mathcal{E}^{\mathrm{d}}, \tag{5}$$

where v^{d} is the GIC-induced voltage magnitude, I^{d}_ℓ is the GIC flowing on the line $\ell \in \mathcal{E}^{\mathrm{d}}$, γ_ℓ is the line conductance, and ξ_ℓ is the GIC-induced voltage source.

Installing a blocking device disconnects the transformer neutral from a substation and changes the conductance matrix. To model this, the GIC balance equations are introduced:

$$\sum_{\ell \in \mathcal{E}^{d-}_m} I^{\mathrm{d}}_\ell - \sum_{\ell \in \mathcal{E}^{d+}_m} I^{\mathrm{d}}_\ell = a_m v^{\mathrm{d}}_m (1 - z_m),\ \forall m \in \mathcal{N}^{\mathrm{d}}, \tag{6}$$

where $\mathcal{E}^{d-}_m$ and $\mathcal{E}^{d+}_m$ are sets of incoming and outgoing lines connected to $m \in \mathcal{N}^{\mathrm{d}}$, a_m is the inverse of ground resistance, and z_m is the binary variable representing the installation of the blocking device, namely $z_m = 1$ if a device is installed at $m \in \mathcal{N}^{\mathrm{d}}$. Eq. (6) deduct the effect of a_m if a device is installed at m. For notation brevity, we set $a_m = 0$ for $m \in \mathcal{N}^{\mathrm{d}} \setminus \mathcal{N}^{\mathrm{s}}$ to ensure that the binary variables z_m are defined only for $m \in \mathcal{N}^{\mathrm{s}}$ where $\mathcal{N}^{\mathrm{s}}$ is a set of substations. To limit the number of blocking devices, we introduce a bound:

$$\sum_{m \in \mathcal{N}^{\mathrm{s}}} z_m \le V, \tag{7a}$$

$$z_m \in \{0,1\},\ \forall m \in \mathcal{N}^{\mathrm{s}}. \tag{7b}$$

where V is the budget for the installation.

5) Effective GIC computation: The GIC in Eq. (5) is used to calculate the effective GIC in Eq. (4a) through the following absolute-value equations for different types of transformers:

$$I^{\mathrm{eff}}_e = |\Theta_e|,\ \forall e \in \mathcal{E}^\tau, \tag{8}$$

where

$$\Theta_e = \Big(\frac{N_h I^{\mathrm{d}}_h + N_l I^{\mathrm{d}}_l}{N_h}\Big),\ \text{if } e \text{ is GWye-GWye}, \tag{9a}$$

$$\Theta_e = \Big(\frac{N_s I^{\mathrm{d}}_s + N_c I^{\mathrm{d}}_c}{N_s + N_c}\Big),\ \text{if } e \text{ is GWye-GWye Auto}, \tag{9b}$$

$$\Theta_e = I^{\mathrm{d}}_h,\ \text{if } e \text{ is GWye-Delta-GSU}, \tag{9c}$$

where N_h, N_l, N_s, and N_c are the number of turns in the high-side, low-side, series, and common windings, respectively.

The absolute value in Eq. (8) is nonsmooth, which can cause convergence failure in MINLP solvers. To avoid this situation, we apply the equivalent smooth complementarity reformulation [18]–[21]:

$$s^+_e - s^-_e = \Theta_e,\ \forall e \in \mathcal{E}^\tau, \tag{10a}$$

$$I^{\mathrm{eff}}_e = s^+_e + s^-_e,\ \forall e \in \mathcal{E}^\tau, \tag{10b}$$

$$s^-_e \ge 0,\quad s^+_e \ge 0,\quad s^+_e s^-_e \le 0,\ \forall e \in \mathcal{E}^\tau, \tag{10c}$$

where s^+_e and s^-_e are slack variables.

6) MINLP models: Now we can define our MINLP model:

(AC-rect)

$$\min \sum_{k \in \mathcal{G}} (c^{\mathrm{F1}}_k f^{\mathrm{p}}_k + c^{\mathrm{F2}}_k (f^{\mathrm{p}}_k)^2) + \sum_{i \in \mathcal{N}} \kappa (l^{\mathrm{p+}}_i + l^{\mathrm{p-}}_i + l^{\mathrm{q+}}_i + l^{\mathrm{q-}}_i)$$

$$\text{s.t. } Eq.\ (1) - Eq.\ (7), Eq.\ (9), Eq.\ (10),$$

where $(c^{\mathrm{F1}}_k, c^{\mathrm{F2}}_k)$ represent cost coefficients associated with generating power at $k \in \mathcal{G}$, and κ represents the unit penalty cost for power imbalance.

III. Heuristic Algorithms

In this section we propose a new heuristic approach for the MINLP model described in Section II, which we call a three-block ADMM algorithm with a binary subproblem, which we will refer to as 3ADMM-B. We also show how a stochastic learning approach can be applied to our problem for comparison purposes.

A. Three-Block Alternating Direction Method of Multipliers

ADMM [22], [23] is typically applied to convex, continuous optimization problems that can be decomposed into two blocks. The method is related to augmented Lagrangian methods and consists of solving a sequence of alternating optimization problems followed by a first-order multiplier update. In contrast, we apply ADMM to a discrete optimization problem. The proposed 3ADMM-B is derived by exploiting the structure of the problem; thus it is a problem-specific algorithm.

First, we observe that the AC and DC network formulations are connected through the effective GIC variables $\{I^{\mathrm{eff}}_e\}_{e \in \mathcal{E}^\tau}$ in Eq. (4) and Eq. (10b). By introducing auxiliary variables I^{ac} and I^{dc}, we separate constraints for the AC network from those for the DC network:

$$g^{\mathrm{ac}}(x, I^{\mathrm{ac}}) \le 0, \tag{11a}$$

$$g^{\mathrm{dc}}(y, z, I^{\mathrm{dc}}) \le 0, \tag{11b}$$

$$I^{\mathrm{dc}}_e = I^{\mathrm{ac}}_e \in [0, \overline{I}_e],\ \forall e \in \mathcal{E}^\tau, \tag{11c}$$

where Eq. (11a) and Eq. (11b) represent constraints for AC and DC networks, respectively, and Eq. (11c) represents consensus constraints. Note that x and y are continuous local variables while z is a binary vector that should satisfy Eq. (7).

Second, we introduce auxiliary variables z^{b} to remove the binary restriction from the DC network:

$$z^{\mathrm{b}}_i = z_i,\ \forall i \in [S], \tag{12a}$$

$$z^{\mathrm{b}}_i \in \{0,1\},\quad z_i \in [0,1],\ \forall i \in [S], \tag{12b}$$

$$\sum_{i=1}^{S} z^{\mathrm{b}}_i \le V, \tag{12c}$$

where $S := |\mathcal{N}^{\mathrm{s}}|$. We note that the consensus constraints Eq. (12a) ensure that the continuous copy agrees with the binary choices. The MINLP model is written in the following form:

$$\min f(x)$$

$$\text{s.t. } Eq.\ (11a) - Eq.\ (11c), Eq.\ (12a) - Eq.\ (12c),$$

where f corresponds to the objective function of `(AC-rect)`.

By introducing dual variables λ and μ associated with Eq. (12a) and Eq. (11c), respectively, the augmented Lagrangian is given by

$$\begin{aligned}\max_{\lambda,\mu}\ \min_{z,z^{\mathrm{b}},I}\ & f(x)+\langle\lambda, z^{\mathrm{b}}-z\rangle+\langle\mu, I^{\mathrm{dc}}-I^{\mathrm{ac}}\rangle \\ & +\frac{\rho}{2}\Big\{\|z^{\mathrm{b}}-z\|^2+\|I^{\mathrm{dc}}-I^{\mathrm{ac}}\|^2\Big\} \\ & \text{s.t. } Eq.\ (11a), Eq.\ (11b), Eq.\ (12b), Eq.\ (12c),\end{aligned} \tag{13}$$

and we now consider an approach that solves (13) instead of `(AC-rect)`. In the tth iteration of the proposed 3ADMM-B, the first-block subproblem is given by

$$\begin{aligned}\min_{z^{\mathrm{b}}\in\{0,1\}^S}\ & \langle\lambda^{(t)}, z^{\mathrm{b}}\rangle+\frac{\rho}{2}\|z^{\mathrm{b}}-z^{(t)}\|^2 \\ \text{s.t.}\ & Eq.\ (12c),\end{aligned} \tag{14}$$

the second-block subproblem is given by

$$\begin{aligned}\min_{z\in[0,1]^S, I^{\mathrm{dc}}\in[0,\overline{I}]}\ & -\langle\lambda^{(t)}, z\rangle+\langle\mu^{(t)}, I^{\mathrm{dc}}\rangle \\ & +\frac{\rho}{2}\Big\{\|z^{\mathrm{b}(t+1)}-z\|^2+\|I^{\mathrm{dc}}-I^{\mathrm{ac}(t)}\|^2\Big\} \\ \text{s.t.}\ & Eq.\ (11b),\end{aligned} \tag{15}$$

the third-block subproblem is given by

$$\begin{aligned}\min_{I^{\mathrm{ac}}\in[0,\overline{I}]}\ & f(x)-\langle\mu^{(t)}, I^{\mathrm{ac}}\rangle+\frac{\rho}{2}\|I^{\mathrm{dc}(t+1)}-I^{\mathrm{ac}}\|^2 \\ \text{s.t.}\ & Eq.\ (11a),\end{aligned} \tag{16}$$

and the dual update is given by

$$\lambda^{(t+1)}=\lambda^{(t)}+\rho(z^{\mathrm{b}(t+1)}-z^{(t+1)}), \tag{17a}$$

$$\mu^{(t+1)}=\mu^{(t)}+\rho(I^{\mathrm{dc}(t+1)}-I^{\mathrm{ac}(t+1)}). \tag{17b}$$

We note that Eq. (15) and Eq. (16) are NLP models with convex quadratic objective functions that are easy to solve, while Eq. (14) is a convex quadratic program with binary variables that is easy to solve, as pointed out in the next remark.

Remark 1. *Since z is binary, we have $\|z\|^2=\langle\mathbf{1}, z\rangle$, where $\mathbf{1}$ is a vector with all components being* 1. *Therefore, Eq.* (14) *can be rewritten as follow:*

$$\begin{aligned}\min_{z\in\{0,1\}^S}\ & \sum_{i=1}^{n}\big(\frac{\rho}{2}+\lambda_i^{(t)}-\rho z_i^{(t)}\big)z_i \\ \textit{s.t.}\ & Eq.\ (12c),\end{aligned}$$

which is a binary knapsack problem whose constraint coefficients are all one. Therefore, an optimal solution can be obtained greedily, as described in lines 9–17 of Alg. 1. Specifically, we first sort the objective coefficient in an increasing order, namely, $\widehat{c}_{i_1}\le\ldots\le\widehat{c}_{i_S}$, and sequentially set $z_j=1$ if $\widehat{c}_{i_j}<0$ for $j\in\{i_1,\ldots,i_S\}$ until the budget V is consumed.

In Alg. 1 we describe the proposed 3ADMM-B algorithm, composed of the three subproblems and dual updates as in lines 3, 4, 5, and 6, respectively. We set the termination criterion based on the normalized primal and dual residuals, as described in [24]. That is, the algorithm is terminated at iteration t if the following holds:

$$\max(p^{(t)}, d^{(t)})<\epsilon, \tag{18}$$

where ϵ is the tolerance of our algorithm and $p^{(t)}$ and $d^{(t)}$ are normalized primal and dual residuals computed at the tth iteration, respectively, given as

$$p^{(t)}:=\frac{\|v^{(t)}-u^{(t)}\|}{\max(\|u^{(t)}\|,\|v^{(t)}\|)},\quad d^{(t)}:=\frac{\rho\|u^{(t)}-u^{(t-1)}\|}{\|w^{(t)}\|}$$

$$v^{(t)}:=\begin{bmatrix}z^{\mathrm{b}(t)}\\ I^{\mathrm{dc}(t)}\end{bmatrix},\quad u^{(t)}:=\begin{bmatrix}z^{(t)}\\ I^{\mathrm{ac}(t)}\end{bmatrix},\quad w^{(t)}:=\begin{bmatrix}\lambda^{(t)}\\ \mu^{(t)}\end{bmatrix}.$$

Algorithm 1 Three-block ADMM with bianry (3ADMM-B)

1: Initialization: $t\leftarrow 0$, $\lambda^{(t)}$, $\mu^{(t)}$, $z^{(t)}$, $I^{\mathrm{ac}(t)}$
2: **while** not converged **do**
3: Compute $z^{\mathrm{b}(t+1)}\leftarrow\texttt{closed}(\rho,\lambda^{(t)},z^{(t)})$
4: Compute $z^{(t+1)}$ and $I^{\mathrm{dc}(t+1)}$ by solving Eq. (15)
5: Compute $I^{\mathrm{ac}(t+1)}$ by solving Eq. (16)
6: Update duals by Eq. (17)
7: **end while**
8: Return $z^{\mathrm{b}(T+1)}$

`closed`(ρ,λ,z^c):
9: Initialization: $z_i=0$ for all $i\in[S]$ and budget $B\leftarrow V$
10: Define $\widehat{c}_i:=\frac{\rho}{2}+\lambda_i-\rho z_i^{\mathrm{c}}$ for all $i\in[S]$
11: Sort elements of $\widehat{c}$ such that $\widehat{c}_{i_1}\le\ldots\le\widehat{c}_{i_S}$
12: **for** $j\in\{i_1,\ldots,i_S\}$ **do**
13: **if** $\widehat{c}_j<0$ and $B>0$ **then**
14: $z_j\leftarrow 1$ and $B\leftarrow B-1$
15: **end if**
16: **end for**
17: Return z

B. Stochastic learning approach

We also apply stochastic learning for binary optimization [25] to our problem. This heuristic finds binary solutions by sampling from a joint multivariate Bernoulli distribution whose probabilities are updated iteratively. It has the advantage that we can easily sample from the final distribution to explore possible alternative solutions, whereas 3ADMM-B is deterministic and produces only a single solution.

To describe the SL approach, we write `(AC-rect)` as

$$\min_{z\in\mathcal{Z}} F(z), \tag{19a}$$

where

$$\mathcal{Z}:=\Big\{z\in\{0,1\}^S:\sum_{i=1}^{S}z_i\le V\Big\} \tag{19b}$$

and $F(z)$ is the optimal value of an NLP model resulting from fixing binary variables in `(AC-rect)` to some value $z\in\mathcal{Z}$.

The existing SL approach [25] has been developed for solving $\min_{z\in\{0,1\}^S} F(z)$ (e.g., Eq. (19) without the constraint):

$$p^* = \arg\min_{p\in[0,1]^S} \Phi(p) := \mathbb{E}_{z\sim\mathbb{P}(z|p)}[F(z)] = \sum_{k=1}^{2^S} P(\hat{z}^k|p)F(\hat{z}^k), \quad (20)$$

where $\mathbb{P}(z|p)$ represents a joint multivariate Bernoulli distribution with the probability mass function, $P(z|p) := \prod_{i=1}^{S} p_i^{z_i}(1-p_i)^{1-z_i}$. Equation (20) is different from the original problem in that it aims to optimize probabilities $\{p_1,\ldots,p_S\}$ associated with binaries $\{z_1,\ldots,z_S\}$, leading to heuristic solutions. Also, Eq. (20) can be considered as a machine learning model with 2^S number of data points. Thus, one can utilize stochastic gradient descent (SGD) types of algorithms for solving Eq. (20). For more details on the existing SL approach, we refer the reader to [25].

In this application, however, the existing approach cannot be immediately utilized because z sampled from the distribution may not satisfy the budget constraint $\sum_{i=1}^{S} z_i \le V$. To address this issue, we first sort the probabilities in a decreasing order, namely, $p_{i_1} \ge \ldots \ge p_{i_S}$, and sample z_j for all $j \in \{i_1,\ldots,i_S\}$ until the budget V is consumed. The proposed sampling is described in lines 3 and 9–18 of Alg. 2. We set the termination criterion based on the norm of gradient, namely, $g^{(t)} < \epsilon$, where ϵ is a tolerance level; and we set the diminishing step size $\eta^{(t)} = a/t$, where $a > 0$ is some constant.

IV. Numerical Experiments

In this section we numerically demonstrate that the proposed heuristic approaches provide good-quality solutions within reasonable computation time, much faster than existing MINLP solvers (e.g., SCIP [26] and Juniper [27]). To achieve this, we employ our proposed approach and established solvers to compute solutions for `(AC-rect)` within a maximum time limit of 1 hour. We then assess solution quality by solving an NLP model that arises from fixing binary variables in the MINLP model to the obtained solutions. Based on the EPRI-21 and UIUC-150 test systems, as described in [17], we designed case studies by varying the magnitude of E-field $E \in \{5, 10, 15, 20\}$ V/km while keeping the E-field direction fixed at 45 degrees. For the EPRI-21 and UIUC-150 system, which have 8 and 98 substations, respectively, each of these substations is a potential location for installing a blocking device. For illustration of the methodology, we set the budget as $V = 3$ for EPRI-21 and $V = 30$ for UIUC-150, with the choice of V proportional to the size of the network.

We used Julia 1.8.1. for writing `(AC-rect)` via JuMP [28] and implementing the heuristic approaches. For all experiments, we used Bebop, a 1024-node computing cluster (each computing node has 36 cores with Intel Xeon E5-2695v4 processors and 128 GB DDR4 of memory) at Argonne National Laboratory. With this computing resource, we solved `(AC-rect)` using our heuristic approach and well-established solvers, each of which is executed sequentially.

Algorithm 2 Stochastic learning approach

1: Initialization: probability $p^{(1)}$, step size $\eta^{(1)}$, sample size N, and set $t \leftarrow 1$
2: **while** not converged **do**
3: Sample N scenarios of $\hat{z} \leftarrow$ `sample`$(p^{(t)})$
4: Compute a gradient:

$$g^{(t)} \leftarrow \frac{1}{N}\sum_{k=1}^{N} F(\hat{z}^k)\Big\{\sum_{i=1}^{S}\Big(\frac{\hat{z}_i^k}{p_i^{(t)}} - \frac{1-\hat{z}_i^k}{1-p_i^{(t)}}\Big)\vec{e}_i\Big\} \quad (21)$$

5: Update

$$p^{(t+1)} \leftarrow \text{Proj}_{[0,1]^S}(p^{(t)} - \eta^{(t)} g^{(t)}) \quad (22)$$
$$t \leftarrow t+1$$

6: **end while**
7: Sample N scenarios of $\hat{z} \leftarrow$ `sample`$(p^{(t+1)})$

`Sample`(p):
8: Initialization: $z_i = 0$ for all $i \in [S]$ and budget $B \leftarrow V$.
9: Sort elements of p such that $p_{i_1} \ge \ldots \ge p_{i_S}$
10: **for** $j \in \{i_1,\ldots,i_S\}$ **do**
11: Sample z_j from the Bernoulli distribution $\mathbb{P}(z|p_j)$
12: **if** $z_j = 1$ **then**
13: $B \leftarrow B - 1$
14: **end if**
15: Break if $B = 0$
16: **end for**
17: Return z

A. Motivating examples

To motivate the development of heuristic approaches, we demonstrate that the optimal placement of blocking devices allows the power system to operate during severe GMDs with a smaller number of blockers, significantly reducing placement cost. We also show that this problem is computationally challenging mainly because of the presence of binary variables.

First, we employ the open-source MINLP solver SCIP to solve `(AC-rect)` using instances constructed by varying the E-field magnitude E within the EPRI-21 system. The results, consisting of the selected substations for installing blocking devices, are reported in Table I. By solving NLP models derived from fixing the binary variables in `(AC-rect)` to the obtained solutions, we compute the load-shedding penalty and power generation cost in Fig. 3 (labeled as "Sol"). This is compared with scenarios where no blocking device is present ("None"), as well as when all substations have blocking devices ("All"). For each E value, installing devices on substations indicated in Table I mitigates the load-shedding penalty while preserving the power generation cost. This signifies that the solutions produced by SCIP within the 1-hour time limit can effectively alleviate the adverse effects of GIC on the power grid, despite not being optimal. We note that although installing blocking devices for all substations eliminates load shedding, the associated installation expenses

can be significant. This situation highlights the necessity of identifying optimal sites for placing these devices.

Unfortunately, solving these MINLP models to optimality is computationally intractable. The solutions reported in Table I are incumbent solutions only obtained within the imposed time limit. The corresponding solution gaps are outlined in Fig. 4. Notably, for the EPRI-21 system, smaller gaps are apparent when $E \leq 15$, while the gap becomes considerably larger at $E = 20$. For the larger UIUC-150 system, the gap is even more pronounced. This underscores the necessity to develop heuristic methods capable of generating high-quality solutions within reasonable computational time.

TABLE I: Set of substations to install blocking devices produced by solving `(AC-rect)` using SCIP.

E [V/km]	5	10	15	20
Substations	$\{3,8\}$	$\{5,6,8\}$	$\{1,6,8\}$	$\{2,6\}$

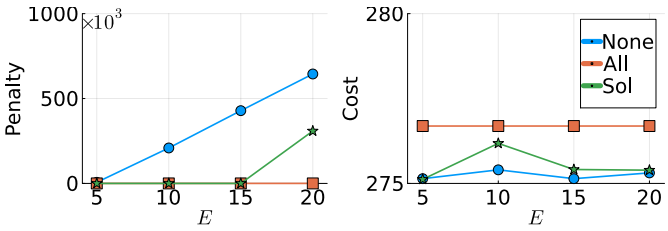

Fig. 3: Effect of installing devices on the load-shedding penalty (left) and the power generation cost (right).

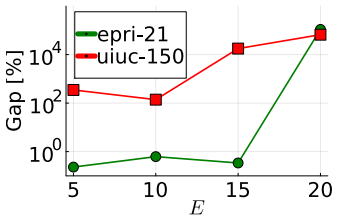

Fig. 4: Gap computed at the time limit of 1 hour.

B. Comparison of heuristic approaches

In this section we numerically show that the proposed heuristic approaches provide superior solution quality compared with existing MINLP solvers. To this end, we first solve `(AC-rect)` constructed by varying $E \in \{5, 10, 15, 20\}$ on the UIUC-150 system by our approaches (i.e., 3ADMM-B and SL), SCIP, and Juniper, respectively. To compare quality of solutions (i.e., where to place devices), we solve an NLP model derived from fixing the binary variables in `(AC-rect)` using the solutions, and we then report the resulting objective values in Table II. Additionally, we provide information on the total time required for computation and evaluation in Table III. The outcomes reveal that the solutions obtained through our heuristic approaches exhibit lower objective values in comparison with solutions generated by SCIP and Juniper, all within a 1-hour time limit. Notably, the enhanced quality of solutions by 3ADMM-B and SL is achieved within computation times of approximately 1 and 18 minutes, respectively. While the 3ADMM-B approach is generally faster than stochastic learning, the stochastic learning approach provides benefits in situations where it is necessary to explore the solution space of near-optimal solutions. Further details regarding these two approaches will be discussed in the subsequent sections.

TABLE II: Comparison of heuristic approaches with respect to the objective value.

E [V/km]	5	10	15	20
SCIP	3029.22	1605.57	122291.70	458847.88
Juniper	3029.22	4111.43	122291.69	458817.29
SL	2232.33	3078.49	5058.66	15117.19
3ADMM-B	3178.71	3178.68	3178.64	3178.61

TABLE III: Comparison of heuristic approaches with respect to the computation time in minutes (TimeLimit=1 hour).

E [V/km]	5	10	15	20
SCIP	TimeLimit	TimeLimit	TimeLimit	TimeLimit
Juniper	TimeLimit	TimeLimit	TimeLimit	TimeLimit
SL	16.1	17.4	17.4	17.7
3ADMM-B	1.1	0.8	0.5	0.9

C. Details on 3ADMM-B

In this section we provide details on 3ADMM-B. The ADMM penalty parameter ρ is a hyperparameter that should be tuned for better performance in practice. We utilize the normalized residual balancing (NRB) technique [24] to adaptively choose the value of ρ in every iteration t of the algorithm. Specifically, for given $\beta, \tau \in \mathbb{R}_+$ and the primal and dual residuals $p^{(t)}, d^{(t)}$, we update ρ as follows:

$$\rho^{(t+1)} \leftarrow \begin{cases} \rho^{(t)}\tau & \text{if } p^{(t)} > \beta d^{(t)} \\ \rho^{(t)}/\tau & \text{if } p^{(t)} < \beta d^{(t)}. \end{cases} \tag{23}$$

To see the effect of the NRB technique on the convergence, we solved the UIUC-150 test instance when $E = 5$ and report how the primal and dual residuals behave in Fig. 5. Specifically, with a constant $\rho = 10^2$, 73 iterations are consumed to solve the instance, while it takes only 19 iterations when NRB with $\rho^{(0)} = 10^2$, $\beta = 2$, and $\tau = 10$ is used.

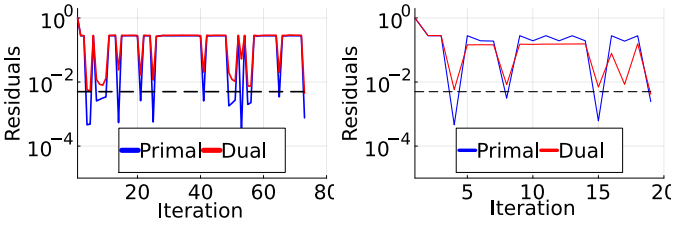

Fig. 5: Effect of the NRB technique on the convergence.

D. Details on SL

In this section we present details on the SL approach. First, we solved the EPRI-21 test instance, which has 8 substations, namely, candidate locations for installing blocking devices, when $E = 5$ V/km. In Fig. 6 we report how the the solutions,

namely, probabilities $\{p_1^{(t)}, \ldots, p_8^{(t)}\}$ in Eq. (21), change over iterations and the norm of gradients (i.e., $\|g^{(t)}\|$ in Eq. (21)). As reported, the solutions started from the initial values of 0.5 change over iterations. For example, the probability of placing a blocking device at substation 8 reaches 1 upon termination, indicating that substation 8 should be chosen as an installation site. For the remaining substations, the probabilities at the termination (i.e., 10th iteration where the norm of the gradient diminishes to zero) are used to determine whether or not to proceed with installation.

The number, N, of samples can be linked to the batch size in the mini-batch SGD, a widely used learning algorithm. As N increases, the algorithm's performance approaches that of a standard gradient descent algorithm. With a larger N, however, the computation time per iteration increases since it entails computing the full or true gradient. In our case, where the objective is to obtain solutions within a 1-hour time limit, we restrict N to be small. In Fig. 7 we illustrate the impact of N on total iterations, average time per iteration, and total time. As anticipated, higher values of N reduce the overall number of iterations needed for termination because of better solution quality per iteration, but this comes at the cost of longer computation time. The choice of N significantly influences the algorithm's performance, necessitating tuning based on the specific application's requirements.

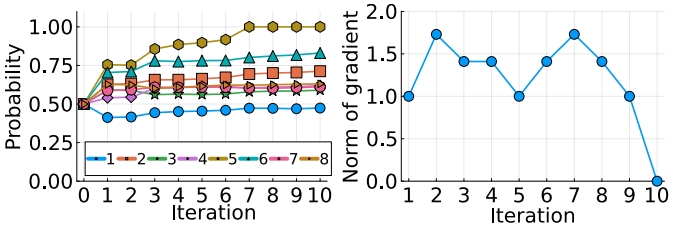

Fig. 6: Variations of solutions (left) and the norm of gradients (right).

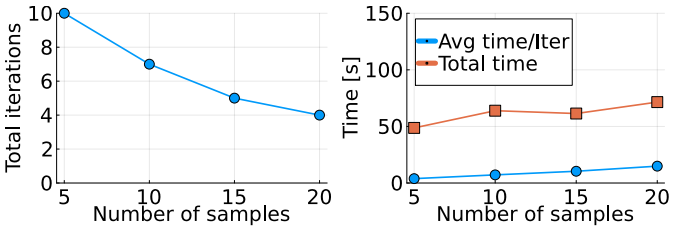

Fig. 7: Effect of the number N of samples used in SL on computation.

V. Conclusion and Future Work

In this paper we derived a MINLP model that mathematically represents the GIC-BDP problem, and we proposed a heuristic algorithm by exploiting the structure of the problem. As opposed to existing models that employ nonsmooth absolute-value equations to calculate effective GIC and intricate nonlinear, nonconvex equations involving trilinear terms with trigonometric functions to compute the amounts of power flow in transmission systems, we have formulated an alternative MINLP model to circumvent potential numerical instability concerns inherent in MINLP solvers. This is achieved by employing a complementarity reformulation technique to smooth out the absolute-value equations. Instead of solving the model using MINLP solvers, which often require substantial time due to the problem's inherent complexity, we have proposed a new heuristic algorithm, 3ADMM-B, that exploits the decomposition of the overall model into three segments. This approach renders each subproblem considerably simpler to solve. We also compared 3ADMM-B with a stochastic learning algorithm that optimizes the probability of GIC blocker placement. Compared with conventional solvers, the heuristics yield solutions of superior quality in significantly shorter timeframes. While 3ADMM-B is typically faster than the stochastic learning approach, the latter allows us to sample from the optimal probability distribution, allowing us to explore possible alternative solutions of similar quality.

As future work, we plan to integrate line switching decisions into the GIC-BDP problem, which serve to effectively counteract the detrimental effects of GIC on power grids by selectively deactivating specific transmission lines. In contrast to the installation of blocking devices, line-switching decisions can be readily modified to enhance overall performance. To address this, we intend to structure the problem as a two-stage optimization process, where we determine the optimal placement of blocking devices in the first stage and make line-switching decisions in the second stage. Given the prompt feasibility of line switching in practical scenarios, we intend to leverage machine learning methodologies to pretrain a model that will provide real-time recommendations on which lines to activate. In consideration of this approach, the heuristic methods proposed in this paper can be employed to generate a collection of training datasets.

Acknowledgments

The work was jointly funded by the U.S. Department of Energy's Office of Electricity Advanced Grid Modeling program and the U.S. Department of Energy's Office of Science Scientific Discovery Through Advanced Computing (SciDAC) program under the project "Space Weather Mitigation Planning."

References

[1] J. G. Kappenman et al. GIC Mitigation: A Neutral Blocking/Bypass Device to Prevent the Flow of GIC in Power Systems. *IEEE Transactions on Power Delivery*, 6(3):1271–1281, 1991.

[2] A. Barnes et al. A review of the gic blocker placement problem. *arXiv preprint arXiv:2402.07302*, 2024.

[3] https://www.dhs.gov/science-and-technology/electromagnetic-pulse-empgeomagnetic-disturbance.

[4] NERC. Effects of Geomagnetic Disturbances on the Bulk Power System System. Technical report, North American Electric Reliability Corporation, 2012.

[5] A. K. Barnes et al. The Risk of Hidden Failures to the United States Electrical Grid and Potential for Mitigation. In *Proc. of the 2021 IEEE 53rd North American Power Symposium*, Nov. 2021.

[6] A. Mate et al. Relaxation Based Modeling of GMD Induced Cascading Failures in PowerModelsGMD.jl. In *Proceedings of the 2021 IEEE/PES 53rd North American Power Symposium*, 2021.

[7] R. Zhang et al. Machine learning-aided enhancement of power grid resilience to electromagnetic pulse strikes. In *2022 North American Power Symposium (NAPS)*, pages 1–6, 2022.

[8] H. Zhu et al. Blocking Device Placement for Mitigating the Effects of Geomagnetically Induced Currents. *IEEE Trans. on Power Systems*, 30(4):2081–2089, 2014.

[9] A. H. Etemadi et al. Optimal Placement of GIC Blocking Devices for Geomagnetic Disturbance Mitigation. *IEEE Transactions on Power Systems*, 29(6):2753–2762, 2014.

[10] Y. Liang et al. Optimal Blocker Placement for Mitigating the Effects of Geomagnetic Induced Currents Using Branch and Cut Algorithm. In *2015 North American Power Symposium (NAPS)*, pages 1–6, 2015.

[11] A. Rezaei-Zare et al. Optimal placement of gic blocking devices considering equipment thermal limits and power system operation constraints. *IEEE Transactions on Power Delivery*, 33(1):200–208, 2017.

[12] Y. Liang et al. Optimal Blocking Device Placement for Geomagnetic Disturbance Mitigation. *IEEE Transactions on Power Delivery*, 34(6):2219–2231, 2019.

[13] X. Ning et al. Research on optimal placement for gic mitigation with blocking device. In *IOP Conference Series: Materials Science and Engineering*, volume 533, page 012042. IOP Publishing, 2019.

[14] S. Wang et al. Optimal blocking devices placement for geomagnetic disturbance mitigation based on sensitivity of induced geoelectric fields. *IEEE Access*, 10:132814–132821, 2022.

[15] M. Lu et al. Optimal Transmission Line Switching Under Geomagnetic Disturbances. *IEEE Trans. on Power Systems*, 33(3):2539–2550, 2017.

[16] M. Ryu et al. Algorithms for Mitigating the Effect of Uncertain Geomagnetic Disturbances in Electric Grids. *Electric Power Systems Research*, 189:106790, 2020.

[17] M. Ryu et al. Mitigating the Impacts of Uncertain Geomagnetic Disturbances on Electric Grids: A Distributionally Robust Optimization Approach. *IEEE Transactions on Power Systems*, 37(6):4258–4269, 2022.

[18] M. C. Ferris et al. Engineering and Economic Applications of Complementarity Problems. *Siam Review*, 39(4):669–713, 1997.

[19] R. Fletcher et al. Solving Mathematical Programs with Complementarity Constraints as Nonlinear Programs. *Optimization Methods and Software*, 19(1):15–40, 2004.

[20] H. Scheel et al. Mathematical Programs with Complementarity Constraints: Stationarity, Optimality, and Sensitivity. *Mathematics of Operations Research*, 25(1):1–22, 2000.

[21] A. U. Raghunathan et al. An Interior Point Method for Mathematical Programs with Complementarity Constraints (MPCCs). *SIAM Journal on Optimization*, 15(3):720–750, 2005.

[22] J. Douglas et al. On the Numerical Solution of Heat Conduction Problems in Two and Three Space Variables. *Transactions of the American mathematical Society*, 82(2):421–439, 1956.

[23] J. Eckstein et al. On the Douglas-—Rachford Splitting Method and the Proximal Point Algorithm for Maximal Monotone Operators. *Mathematical Programming*, 55:293–318, 1992.

[24] B. Wohlberg. ADMM Penalty Parameter Selection by Residual Balancing. *arXiv preprint arXiv:1704.06209*, 2017.

[25] A. Attia et al. Stochastic Learning Approach for Binary Optimization: Application to Bayesian Optimal Design of Experiments. *SIAM Journal on Scientific Computing*, 44(2):B395–B427, 2022.

[26] K. Bestuzheva et al. The SCIP Optimization Suite 8.0. ZIB-Report 21-41, Zuse Institute Berlin, December 2021.

[27] O. Kroger et al. Juniper: An Open-Source Nonlinear Branch-and-Bound Solver in Julia. In *Integration of Constraint Programming, Artificial Intelligence, and Operations Research Conference*, pages 377–386, 2018.

[28] M. Lubin et al. JuMP 1.0: Recent Improvements to a Modeling Language for Mathematical Optimization. *Mathematical Programming Computation*, 2023.